Journal of Catalysis 436 (2024) 115607

Contents lists available at ScienceDirect

Journal of Catalysis

journal homepage: www.elsevier.com/locate/jcat

Research article

Phosphorus-modification of Pt/Al_2O_3 catalysts improves dispersion and cycloalkane dehydrogenation activity

Abelina Ellert [a], Felix Herold [b], Magnus Rønning [b], Andreas Hutzler [c], Luca Piccirilli [d], Ton V.W. Janssens [d], Peter N.R. Vennestrøm [d,1], Peter Wasserscheid [a,c,e], Patrick Schühle [a,*]

[a] Institute of Chemical Reaction Engineering, Friedrich-Alexander-Universität Erlangen-Nürnberg, Egerlandstr. 3, 91058 Erlangen, Germany
[b] Department of Chemical Engineering, Norwegian University of Science and Technology (NTNU), 7491 Trondheim, Norway
[c] Helmholtz Institute Erlangen-Nürnberg for Renewable Energy (IEK-11), Cauerstr. 1, 91058 Erlangen, Germany
[d] Umicore Denmark Aps, Kogle Alle 1, 2970 Hørsholm, Denmark
[e] Forschungszentrum Jülich GmbH, Institute for a Sustainable Hydrogen Economy, Am Brainergy Park 4, 52428 Jülich, Germany

ARTICLE INFO

Keywords:
Heterogeneous catalysis
Doping
Phosphorus
Dehydrogenation
LOHC

ABSTRACT

In this study, we demonstrate that phosphorus-modification of Pt/Al_2O_3 leads to sinter-stable catalysts with improved activity in the dehydrogenation of perhydro benzyltoluene, an attractive liquid organic hydrogen carrier. TEM images show that platinum nanoparticles are stabilized to a size below 1 nm by the P-modification procedure, while unmodified counterparts show considerable sintering after reduction at 600 °C. The modification procedure starts by a simple impregnation of Pt/Al_2O_3 with H_3PO_3, followed by a high temperature treatment above 550 °C. It is crucial to adjust the right P:Pt ratio to reach stabilization of all platinum nanoparticles and thereby high catalytic surface areas. In our dehydrogenation studies, a catalyst with the optimal molar P:Pt ratio of 1.8 shows a 18 % higher activity compared to the unmodified sample. Even after treating the catalyst at temperatures up to 900 °C, this activity boost remains. XPS and XRD measurements prove that Pt stays in its reduced elemental state, also after P-modification, which is essential for a good dehydrogenation activity. The phosphorus species act as an anchor for the Pt particles on the Al_2O_3 surface, reducing their mobility and preserving small nanoparticles.

1. Introduction

In heterogeneous catalysis, supported metal nanoparticles play a central role in efficiently converting the reactants to the desired products. Platinum (Pt) is one of the most widely used metals in heterogeneous catalysis, applied for a variety of reactions, including hydrogenations or dehydrogenations, that are relevant for chemical hydrogen storage.[1–4] Typically, Pt nanoparticles are anchored onto porous substrates, such as Al_2O_3. The high dispersion of small nanoparticles on the support increases the Pt surface area and the catalytic activity. Moreover, the addition of other metals[5–7] and non-metallic elements as promoters can further increase the catalyst's activity, adjust its selectivity and stabilize the catalyst.[8,9] As an example for a metal promoter, tin (Sn) is recognized for its ability to impede side reactions and the formation of coke, while also enhancing the dispersion of Pt. Consequently, Pt-Sn catalysts show higher activity and selectivity in the production of olefins by alkane dehydrogenation.[10,11].

Sulfur, a strong poison to Pt catalysts when added in large amounts, can be beneficial for the catalyst stability and selectivity, when only incorporated in low quantities. This effect was demonstrated in several reactions, such as alkane reforming and alkane dehydrogenations. [12–15] In the liquid phase dehydrogenation of perhydro dibenzyltoluene, a well-known liquid organic hydrogen carrier (LOHC), S-doping of Pt catalysts leads to an increase in activity. The electronic properties of platinum are modified by sulfur atoms, allowing a faster desorption of the reaction product dibenzyltoluene. Furthermore, low coordinated edge and corner atoms of the Pt nanoparticles, that are responsible for side product formation, are selectively blocked by sulfur species. [15,16].

Here, we refer to a similar LOHC molecule, perhydro benzyltoluene

Abbreviations: LOHC, liquid organic hydrogen carrier; H12-BT, perhydro benzyltoluene; DoDh, degree of dehydrogenation; MF, methyl fluorene.

* Corresponding author.
E-mail address: patrick.schuehle@fau.de (P. Schühle).

[1] Present address: Topsoe A/S, Haldor Topsøes Alle 1, DK-2800 Kgs, Lyngby, Denmark.

https://doi.org/10.1016/j.jcat.2024.115607
Received 10 March 2024; Received in revised form 14 May 2024; Accepted 12 June 2024
Available online 13 June 2024

(H12-BT). Its dehydrogenation forms the desired hydrogen-lean molecule benzyltoluene (H0-BT). Methyl fluorene (MF) is formed by releasing a further hydrogen molecule in the so-called deep dehydrogenation reaction (Scheme 1). It is considered as a first consecutive side product in H12-BT dehydrogenation and can undergo consecutive reactions to heavy aromatic side products.-[17] Therefore, MF is a suitable probe molecule to investigate the selectivity of a LOHC dehydrogenation catalyst. MF formation is provoked at low coordinated Pt sites as the fast desorption of H0-BT is hampered. Adding sulfur as a promoter to block these sites, consequently prevents the formation of side products, and hence the degradation of the LOHC compound.[15].

A major risk of S-modified catalysts in a hydrogen-rich environment is sulfur leaching by formation of H_2S. This leaching effect depends on the thermal treatment of the catalyst during preparation and can occur already at temperatures of 300 °C and is known e. g. from the hydrodenitrogenation reaction, where transition metal sulfide catalysts are applied since decades.[17] As a result, the constant loss of promoter mitigates its positive effect on the catalyst performance and the H_2S formed may contaminate the product gas.

A recent density functional theory study predicts that phosphorus (P) should be able to boost the catalytic activity of Pt in cyclohexane dehydrogenation, in the same manner as sulfur does.[18] Experimental studies reveal that the incorporation of phosphorus enhances product desorption by reducing the bond strength between platinum and adsorbates.[19].

These facts render phosphorus a promising promoter for Al_2O_3-supported Pt catalysts applied in dehydrogenation of LOHCs. So far, only a few studies have been devoted to understanding the effects of P promoters for supported Pt catalysts in dehydrogenation reactions.[19,20] Recently, Kou *et al.* have found that P-modification of Pt/SiO_2 catalysts induces a superior olefin selectivity in propane dehydrogenation as the product desorption is accelerated. The catalyst activity is in turn reduced, as phosphorus oxidizes elemental platinum to Pt^{2+} and triggers the formation of a less active PtP_2 phase.[19].

In this study, we demonstrate the promising effect of P-modification for Al_2O_3-supported Pt catalysts in the dehydrogenation of perhydro benzyltoluene. The P-modified catalysts exhibit strong bonding of phosphorus with no loss of the promoter at synthesis temperatures of up to 900 °C. At the same time, phosphorus improves and stabilizes Pt dispersion, while keeping the metal in its active elemental state. In contrast to previous reports where phosphorus modification lead to a decrease in dehydrogenation activity, the formation of a platinum phosphide phase was not observed for our novel materials. In this context, the Al_2O_3 support plays a decisive role, avoiding the formation of a PtP_2-phase that would occur by reduction of the phosphorus precursor and a consequent oxidation of the platinum species.

2. Experimental

2.1. Materials

In this study we used a γ-Al_2O_3 support material, with a surface area of approximately 140 m^2/g, which was calcined at 500 °C for 4 h in air flow (10 K min^{-1}) before use. $H_2[PtCl_6]\bullet 6H_2O$ (38–40 % Pt, 99.9 %) was purchased from abcr GmbH (Karlsruhe, Germany) and H_3PO_3 (99 %) from Merck KGaA (Darmstadt, Germany).

2.2. *Catalyst* preparation

Pt/Al_2O_3 was prepared by impregnation of Al_2O_3 overnight (16 h) at room temperature with an aqueous solution of $H_2[PtCl_6]\bullet 6\ H_2O$. The solvent was evaporated at 80 °C and 150 mbar. The obtained powder was calcined at 400 °C (10 °C min^{-1}) in air and then either reduced under 10 % H_2/N_2 (500 mln min^{-1}, heating in N_2 at 10 K min^{-1}) in a tubular furnace (Carbolite Gero GmbH & Co. KG, Neuhausen) to obtain an unmodified Pt catalyst or further impregnated with a phosphorus precursor. The impregnation of calcined Pt/Al_2O_3 with H_3PO_3 was conducted overnight (16 h) followed by solvent removal at 80 °C and 150 mbar. The obtained phosphorus-modified catalyst samples were directly reduced in a tubular furnace (10 % H_2/N_2, 500 mln min^{-1}, heating in N_2 at 10 K min^{-1}) without prior calcination.

2.3. *ICP-OES*

The platinum and phosphorus contents in the samples were determined *via* inductively coupled plasma optical emission spectroscopy (ICP-OES). 100 mg of catalyst samples were digested in 10 mL aqua regia (HNO_3:HCl volumetric ratio 4:6) using microwave heating (200 °C) and subsequently diluted to 100 mL with deionized water. The emission spectra of the solutions were conducted on a Ciros CCD by SPECTRO Analytical Instruments GmbH (Kleve, Germany).

2.4. *N_2 physisorption*

To determine textural properties, such as specific surface area and pore volume, N_2 physisorption was performed at −196 °C on a Quadrasorb SI by Quantachrome Instruments. Prior to measurement, the samples were degassed and dried for 12 h at 250 °C under vacuum (0.01 mbar) to remove any residues from the surface. The specific surface area was determined by the BET method in a relative pressure range of 0.05–0.2. The total pore volume was determined at $p/p_0 = 0.99$.

2.5. *Electron microscopy*

For the determination of platinum particle size distributions, high-angle annular dark field scanning transmission electron microscopy (HAADF-STEM) combined with energy dispersive X-ray spectroscopy (EDXS) was conducted on a Talos F200i by Thermo Fisher Scientific. For the evaluation of particle size distributions, the projected areas of 150 to 200 particles were evaluated. The volume-area-mean particle size is calculated as $d_{VA} = \sum n_i d_i^3\ (\sum n_i d_i^2)^{-1}$, where n_i is the number of particles with diameter d_i.

2.6. *CO pulse chemisorption*

For the investigation of CO adsorption behavior of the catalysts, chemisorption experiments with CO as pulse gas were conducted on an Autochem II 2920 by Micromeritics. Prior to chemisorption, catalyst samples were treated in 10 % H_2/Ar (5 °C min^{-1}, 50 ml min^{-1}, 60 min at 440 °C or 600 °C for Pt/Al_2O_3, 440 or 700 °C for phosphorus-modified

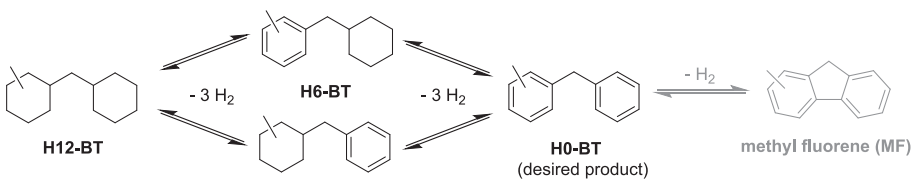

Scheme 1. Reaction scheme of perhydro benzyltoluene (H12-BT) dehydrogenation over intermediate H6-BT to benzyltoluene (H0-BT) with further deep dehydrogenation to methyl fluorene (MF).

catalysts). Pulse chemisorption was performed at 40 °C and with 10 % CO/He. The adsorbed amount of CO was calculated from the difference of dosed and not-adsorbed CO volume assuming ideal gas. The dispersion of Pt was calculated assuming a stoichiometric factor of 1.

2.7. *X-ray diffraction*

In order to determine the morphology of the catalysts, X-ray diffraction (XRD) patterns were recorded using a Pananalytical X-Pert Pro-MD by Philips equipped with a Cu-Kα (wavelength λ of 1.5406 Å) source in a range from 10° to 90° with a scan speed of 0.02° s^{-1}.

2.8. *XPS*

For the investigation of electronic properties and oxidation states of platinum and phosphorus, X-ray photoelectron spectroscopy (XPS) was conducted on a Kratos Analytical Axis Ultra DLD spectrometer using monochromatic Al Kα irradiation (1486.6 eV) operating the anode at 10 kV with an aperture of 700 × 300 µm. Survey scans were recorded with a pass energy of 160 eV, while high-resolution spectra were measured with a pass energy of 20 eV. The energy axis was calibrated by fixing the C1s contribution of adventitious carbon at 284.8 eV.

2.9. *Catalytic testing*

To evaluate the catalytic activity of the catalysts, batch dehydrogenation tests were conducted in a glass set-up consisting of a three-necked 100 mL flask, a two-neck attachment with a metallic hollow cylinder for catalyst storage, and a reflux condenser. A schematic illustration of the set-up can be found in the supporting information (Figure S1). All experiments were performed using 15 g perhydro benzyltoluene (H12-BT, degree of hydrogenation 97.37 %, obtained from hydrogenation of benzyltoluene, benzyltoluene by Eastman Chemical Company,) and a molar H12-BT:Pt ratio of 2000. For a 3 wt% Pt catalyst, this corresponds to 251 mg catalyst. Prior to each experiment, the set-up was flushed with Ar during heating to reaction temperature (250 °C, 1 atm). As soon as the reaction temperature of 250 °C was reached, the inert gas flow was stopped, and the catalyst powder was dropped into the hot liquid. Liquid samples were taken over the course of the reaction (six hours) and analyzed *via* refractive index measurements (DR6100-T by Krüss Optronic GmbH, calibrated with GC) and GC-FID (Shimadzu 2010 Plus; column Rxi-17Sil MS 30 m, 0,25 mm ID, 0.25 µm by Restek). Detailed information on the evaluation of GC-FID data is given in the ESI.

The performance of the catalyst is evaluated using the degree of dehydrogenation (DoDh). The DoDh is defined as the ratio between the actual amount of released hydrogen and the amount of hydrogen that would be released at complete dehydrogenation, corresponding to six H_2 molecules per molecule perhydro benzyltoluene. The H_2 yield in $g_{H2}\ g_{Pt}^{-1}$ was calculated from the DoDh determined by GC analysis *via* Equation (1).

$$Y_{H_2} = \frac{\Delta DoDh \bullet n_{H12-BT} \bullet 12}{m_{Pt}} \quad (1)$$

Here, $\Delta DoDh$ is the difference in degree of dehydrogenation before and after reaction, $n_{H12\text{-}BT}$ the molar amount of perhydro benzyltoluene and m_{Pt} the amount of platinum in gram. The number 12 corresponds to the amount of hydrogen in gram that would be released at complete dehydrogenation per mole of H12-BT. GC analysis is further used to evaluate byproduct formation.

3. Results

To determine the effect of a phosphorus promoter on a Pt/Al_2O_3 catalyst for dehydrogenation of perhydro benzyltoluene, a series of catalyst materials containing 3 wt% Pt and various amounts of phosphorus (up to 2 wt%) were prepared (Table 1). As a second parameter, the reduction temperature of the catalysts after impregnation with H_3PO_3 was varied between 440 and 900 °C. Table 1 gives a list of catalysts investigated in this work (details are listed in Table S1).The ICP-OES results demonstrate that the nominal Pt and P loadings could be achieved without any loss of phosphorus upon reduction at temperatures up to 900 °C (catalyst **3-f**).

The catalytic performance of the P-modified catalysts was evaluated in batch dehydrogenation experiments using perhydro benzyltoluene (H12-BT) as feedstock. Note, that the DoDh, the product content of methyl fluorene and the ratio of H0-, H6- and H12-BT are listed in Table S4 for all dehydrogenation experiments of this study.

In a first set of experiments, the influence of the reduction temperature – applied after P impregnation of the catalysts – on the resulting dehydrogenation activity was studied. All catalysts in this set (catalysts **2** and **3-a** to **3-f**) maintained a constant P:Pt ratio of 1.8. Charted in Fig. 1 a is the accumulated yield of H_2 over reaction time.

The H_2 release is fast at the start of the measurement, as indicated by the steep slope of the curve. As the dehydrogenation proceeds, the concentration of the reactant, and thus the dehydrogenation rate, decrease. To evaluate and compare the activity of different catalysts, we focus on the H_2 yield after 360 min of reaction. The unmodified catalyst that was reduced at 440 °C exhibits a H_2 yield of 67 $g_{H2}\ g_{Pt}^{-1}$. The P-modified counterparts treated at temperatures of 440 and 500 °C reach nearly identical values. By increasing the reduction temperature beyond these temperatures, the Pt-based H_2 yield improves, and reaches a plateau above 80 $g_{H2}\ g_{Pt}^{-1}$ for the catalyst reduced at 600 °C. Interestingly, catalysts prepared under even higher reduction temperatures of up to 900 °C keep the H_2 yield on this high level.

A comparison of the H_2 yield after 360 min with an unmodified Pt catalyst is given in Fig. 1 b. A reduction temperature of 440 °C is the

Table 1
Overview of the catalysts investigated in this work. Nominal and achieved Pt and P loadings on Al_2O_3 after reduction under hydrogen flow at different temperatures (2 h, 500 mln min^{-1}, 10 % H_2/N_2). Areal concentration of P (P_{atoms}/nm^2) calculated based on BET surface area of support material. Standard deviation given for repeatedly prepared catalysts; detailed compositions are shown in Table S1.

No.	Catalyst	Nominal Pt wt.%	Nominal P wt.%	Pt wt.% (ICP–OES)	P wt.% (ICP–OES)	Molar P:Pt ratio	P_{atoms}/nm^2
1-a	Pt red. 440 °C	3	0	3.0	0	0	–
1-b	Pt red. 600 °C	3	0	3.1	0	0	–
2-a	P:Pt 1.0 red. 600 °C	3	0.6	3.1	0.5	1.0	0.7
2	P:Pt 1.8 red. 600 °C	3	0.9	3.0 ± 0.2	0.9 ± 0.0	1.8 ± 0.1	1.2 ± 0.1
2-b	P:Pt 2.5 red. 600 °C	3	1.2	3.3	1.3	2.5	1.7
2-c	P:Pt 4.2 red. 600 °C	3	2.0	3.3	2.2	4.2	3.0
3-a	P:Pt 1.9 red. 440 °C	3	0.9	3.0 ± 0.2	0.9 ± 0.0	1.9 ± 0.1	1.2 ± 0.0
3-b	P:Pt 1.6 red. 500 °C	3	0.9	3.1	0.8	1.6	1.2
3-c	P:Pt 1.8 red. 550 °C	3	0.9	3.1 ± 0.0	0.9 ± 0.0	1.8 ± 0.0	1.2 ± 0.0
3-d	P:Pt 1.8 red. 650 °C	3	0.9	3.1 ± 0.2	0.9 ± 0.0	1.7 ± 0.1	1.2 ± 0.1
3-e	P:Pt 1.8 red. 700 °C	3	0.9	3.1 ± 0.1	1.0 ± 0.1	1.9 ± 0.1	1.3 ± 0.1
3-f	P:Pt 1.9 red. 900 °C	3	0.9	3.0	0.9	1.9	1.2

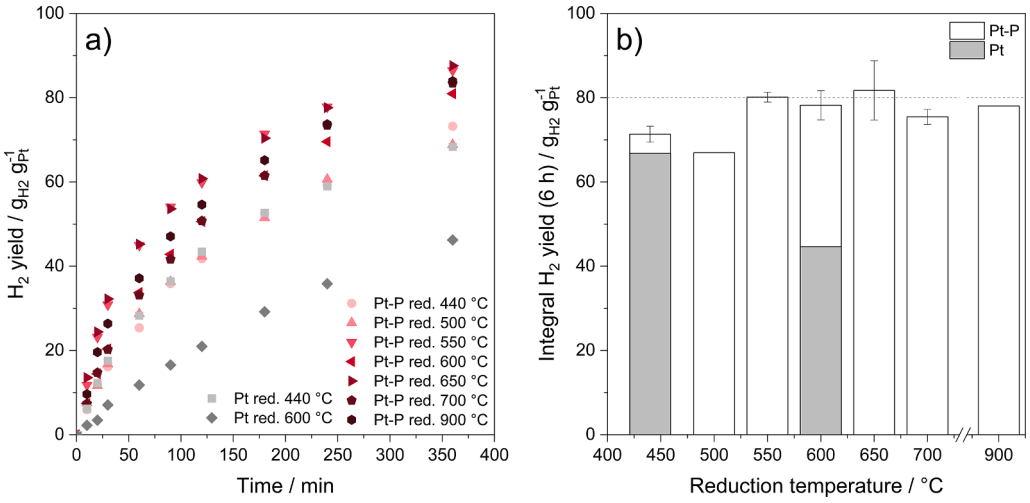

Fig. 1. a) H_2 yield from perhydro benzyltoluene dehydrogenation over time for Pt-P/Al_2O_3 (catalysts **2** and **3-a** to **3-f**) and unmodified Pt/Al_2O_3 (**1-a**, **1-b**) after reduction at temperatures between 440 and 900 °C. Reaction conditions: 250 °C, 1 atm, 15 g H12-BT, molar H12-BT:Pt ratio = 2000. Liquid samples analyzed via refractive index. b) H_2 yield after 360 min of reaction. Liquid samples analyzed via GC-FID. Error determined from repeated dehydrogenation experiments with different catalyst batches.

state-of-the-art to activate such Pt catalysts[21,22], while 600 °C was applied for direct comparison with the Pt-P catalysts in this study (**1-a** and **1-b**). The H_2 yield drops from 67 to 45 g_{H2} g_{Pt}^{-1} when the reduction temperature is increased from 440 to 600 °C and if no phosphorus-modification has taken place beforehand.

Besides reduction temperature, the amount of phosphorus species added during the P-modification procedure could additionally affect the catalyst behavior. Therefore, a variation of the molar P:Pt ratio in the range between 1.0 and 4.2 (catalysts **2** and **2-a** to **2-c**) was conducted for Pt-P catalysts reduced at 600 °C. Their catalytic results are given in Fig. 2 a, showing that the H_2 yield reached by the different catalysts differs already form the start of the reaction. Catalysts with a molar P:Pt ratio of 1.0, 2.5 and 4.2 show a decreased initial slope compared to catalyst **2** with a ratio of 1.8, and consequently achieve lower integral H_2 yields. This is also reflected in higher rates over the whole course of the reaction (Figure S11 a). The pronounced effect of the applied P content becomes visible in Fig. 2 b. The difference in H_2 yield between the catalyst with the optimal P:Pt ratio (1.8), compared to the lowest (1.0) and to the highest (4.2) ratio is a factor of about 1.2 and 2.3, respectively.

The most pronounced effect of phosphorus-modification is therefore found for the catalyst with a P:Pt ratio of 1.8, after reduction at 600 °C (catalyst **2**). The integral H_2 yield after 6 h is 18 % higher than observed for a corresponding unmodified Pt/Al_2O_3 catalyst without phosphorus (catalyst **1-a**).

To elucidate the selectivity of the P-modified Pt catalysts, the formation of methyl fluorene (MF) as a representative byproduct is evaluated. Here, the phosphorus-modified catalyst **2** shows a slightly increased content of methyl fluorene in the liquid at similar degrees of dehydrogenation compared to the unmodified catalysts **1-a** and **1-b** (Fig. 3).

From kinetic investigations of the most active catalyst **2**, an activation energy of 155 kJ mol^{-1} was determined (Figure S9), which is in an expected range when comparing to previous reports of Pt-based catalysts in H12-BT dehydrogenation.[23,24] Furthermore, catalyst **2** was subjected to Soxhlet extraction using cyclohexane after 6 h of dehydrogenation and the recycled catalyst was tested in a second run. Here, no loss in dehydrogenation activity or differences in DoDh or MF-content after 6 h could be identified (Figure S10).

To determine how the P-modification influences particle size distribution, chemical and electronic properties of platinum and results in a higher activity for dehydrogenation, we have investigated the catalysts by several analytical techniques. Comparison of the Al_2O_3 support and the P-modified Pt catalyst **2** (P:Pt = 1.8, red. 600 °C) do not indicate significant changes in the textural properties upon catalyst synthesis.

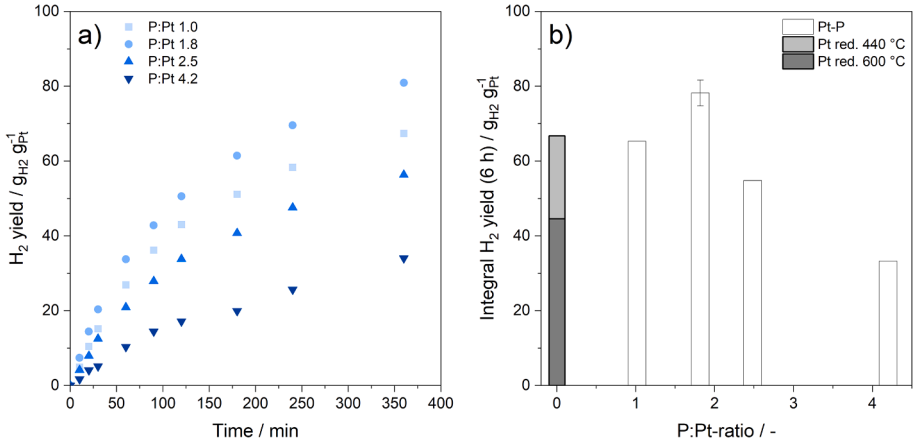

Fig. 2. a) H_2 yield from perhydro benzyltoluene dehydrogenation over time for Pt-P/Al_2O_3 (catalysts **2** and **2-a** to **2-c**) with different molar P:Pt ratios from 1.0 to 4.2. Reaction conditions: 250 °C, 1 atm, 15 g H12-BT, molar H12-BT:Pt ratio = 2000. Liquid samples analyzed via refractive index. b) H_2 yield after 6 h of reaction analyzed via GC-FID. Error determined from repeated dehydrogenation experiments with different catalyst batches.

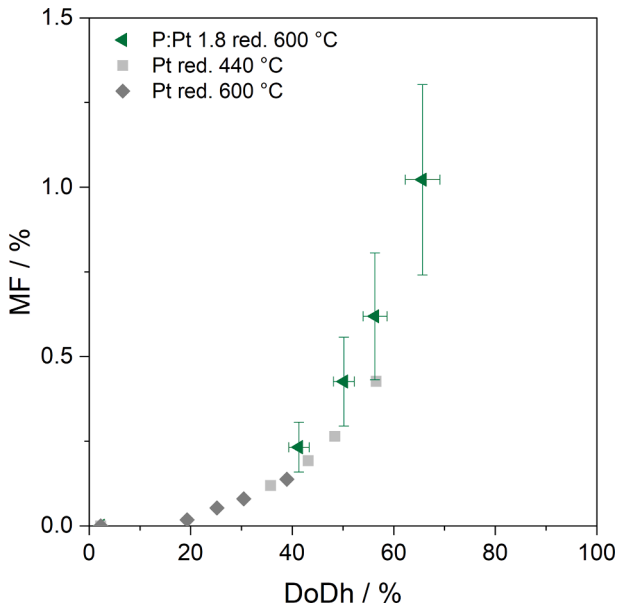

Fig. 3. Methyl fluorene (MF) content in dependency of degree of dehydrogenation (DoDh) for Pt-P/Al_2O_3 (catalyst **2**) and unmodified Pt catalysts (catalysts **1-a** and **1-b**, reduced at 440 or 600 °C, respectively). Reaction conditions: 250 °C, 1 atm, 15 g H12-BT, molar H12-BT:Pt ratio = 2000. Liquid samples analyzed via GC-FID. Error determined from repeated dehydrogenation experiments with different catalyst batches.

The BET surface area, total pore volume and average pore diameters, as determined by N_2 physisorption (see Table S3), are constant at values of about 140 $m^2\ g^{-1}$, 0.5 $cm^3\ g^{-1}$ and 14 nm, respectively.

HAADF-STEM and STEM-EDX analysis were performed to investigate the local distribution of platinum and phosphorus and the particle size distributions on the catalysts. Fig. 4 shows the location of both elements in catalyst **2**. Pt (yellow) and P (red) are homogeneously distributed over the surface of the support. In the unmodified catalyst reduced at 440 °C, Pt is also well distributed and forms small particles of about 1 nm (**1-a**, Figure S2), whereas larger particles of about 5.8 nm on average are observed after reduction at 600 °C (**1–b**, Figure S3). The P-modified catalysts with P:Pt ratios below and above the optimum (here ratios of 1.0 and 2.5, catalysts **2-a** and **2-b**, respectively), show highly dispersed Pt particles of small average particle sizes between 1.1 and 1.2 nm along with a few particles larger than 2.5 nm (Figure S4, Figure S5, Figure S6). The images of these larger particles at non-optimal P loadings clearly visualize that phosphorus is specifically concentrated at the Pt nanoparticles. This aspect remained obscured for catalyst **2** due to the high dispersion, and hints to a preferred location of phosphorus in close proximity to platinum.

Particle size distributions and the volume-area-averaged particle sizes were obtained from HAADF-STEM images. Here, an unmodified Pt catalyst (reduced at 440 and 600 °C, catalysts **1-a** and **1-b**) and a Pt-P catalyst with a molar P:Pt ratio of 1.8 (catalyst **2**) before and after reduction at 600 °C were analyzed. In Fig. 5 a the growth of particles on the unmodified Pt catalyst upon increasing the reduction temperature from 440 to 600 °C is visible, resulting in an increase of the volume-area-mean particle size (d_{VA}) from 1.1 nm (**1-a**) to 5.8 nm (**1-b**). The P-modified catalyst exhibits slightly smaller average particle sizes of 0.9 nm despite the higher reduction temperatures (600 °C), and a narrower distribution compared to the unmodified Pt catalyst reduced at a lower temperature (440 °C). On top of that, particle sizes were decreased in the Pt-P catalyst upon high-temperature reduction compared to the unreduced counterpart (Fig. 5 b).

As can be seen from Table 2, regardless of the P content, the particle sizes of P-modified catalysts are in the 1 nm range despite the high reduction temperatures, compared to the unmodified Pt catalyst reduced at 600 °C (**1-b**). Furthermore, Pt-P catalysts with lower and higher molar P:Pt ratios of 1.0 and 2.5 (catalyst **2-a** and **2-b**, respectively; Figure S6) have a volume-area-averaged particle size of 1.1 and 1.2 nm, respectively (large particles > 5 nm were not considered here due to their small quantity).

CO pulse chemisorption measurements were conducted to investigate the change in the number of Pt surface atoms (Table 3). This can indicate changes in the binding of reactants on P-modified and unmodified catalysts. Particle sizes and dispersions calculated from CO sorption are strongly dependent on the availability and electronic nature of the Pt centers and can potentially deviate from the real particle sizes observed in STEM. Hence, instead of dispersion we report the adsorbed amount of CO per mole Pt to assess changes in the number of available Pt centers.

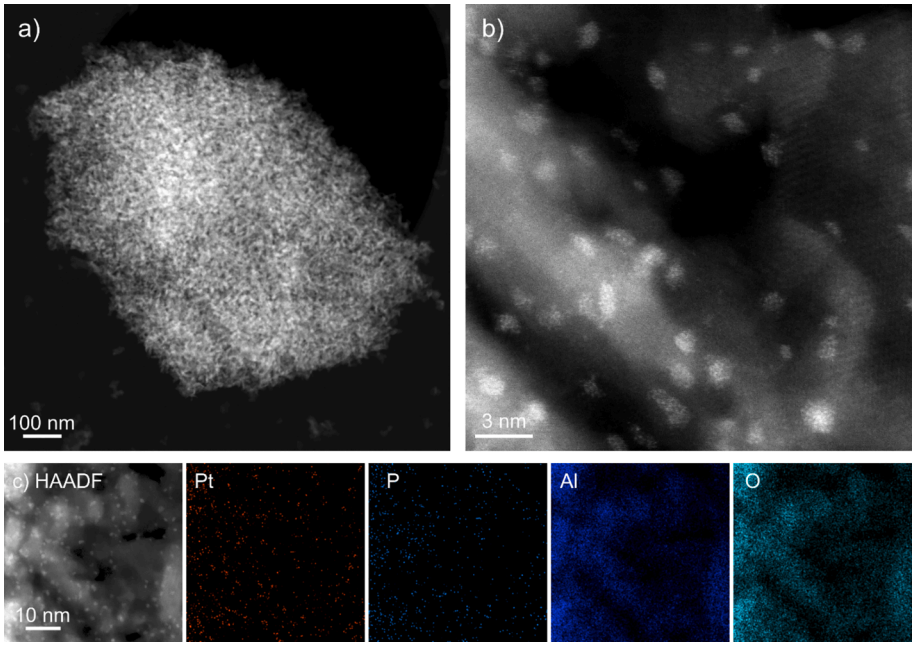

Fig. 4. a) HAADF. b) HAADF. c) HAADF and STEM-EDX-scans of 3 wt% Pt and 0.9 wt% P on Al_2O_3 reduced at 600 °C (molar P:Pt ratio = 1.8, catalyst **2**).

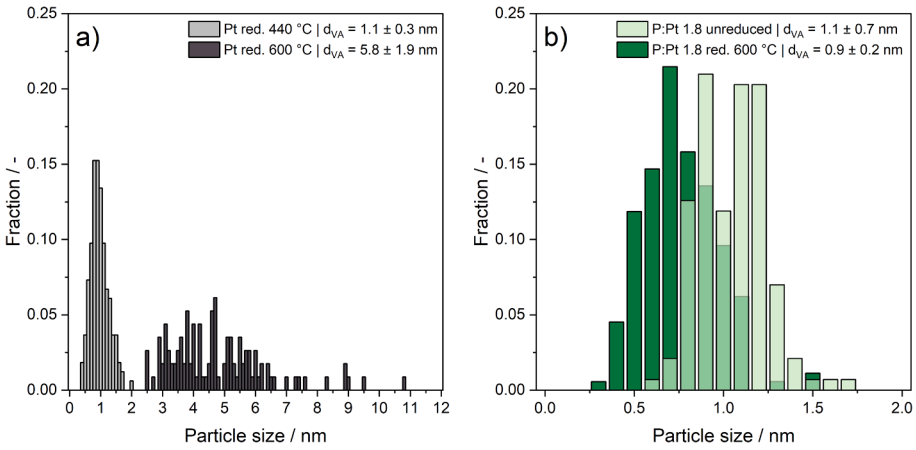

Fig. 5. a) Particle size distributions from HAADF-STEM-images of unmodified pt catalyst reduced at 440 °C (catalyst **1-a**) and 600 °C (catalyst **1-b**). b) Particle size distributions from STEM analysis of Pt-P catalysts with molar P:Pt ratio of 1.8 before and after reduction at 600 °C (catalyst **2**). d_{VA} = volume-area-mean particle size.

Table 2
Average particle sizes of unmodified and P-modified Pt catalysts at different molar P:Pt ratios.

Catalyst	Reduction temperature / °C	Molar P:Pt ratio	Average particle size (STEM) / nm
1-a	440	–	1.1
1-b	600	–	5.8
2-a	600	1.0	1.1
2	600	1.8	0.9
2-b	600	2.5	1.2

Table 3
Amount of adsorbed CO per platinum in CO pulse chemisorption measurements of unmodified and phosphorus-modified 3 wt% Pt catalysts.

	Catalyst	Adsorbed CO / mmol mol_{Pt}^{-1}
1-a	Pt red. 440 °C	572
1-b	Pt red. 600 °C	126
3-a	P:Pt 1.8 red. 440 °C	325
2-a	P:Pt 1.0 red. 600 °C	451
2	P:Pt 1.8 red. 600 °C	429
2-b	P:Pt 2.5 red. 600 °C	255
2-c	P:Pt 4.2 red. 600 °C	283

The chemisorption results show that the highest amount of CO can be adsorbed by the unmodified Pt catalyst reduced at 440 °C (**1-a**). This adsorption capacity drastically decreases by a factor of 4.5 for the same catalyst reduced at 600 °C (**1-b**). The CO adsorption capacity of P-modified catalysts with a P:Pt ratio of 1.8 reduced at 440 (**3-a**) and 600 °C (**2**) is also decreased compared to the unmodified Pt catalyst treated at lower temperatures (**1-a**), but to a lower extent. Furthermore, the adsorption of CO for a Pt-P catalyst is enhanced upon an increase in reduction temperature from 440 to 600 °C. For a lower P:Pt ratio of 1.0 (catalyst **2-a**), the adsorption capacity is about 5 % higher, whereas with increasing P loading (catalyst **2-b** and **2-c**), the CO adsorption capacity further decreases to a level around 270 mmol mol_{Pt}^{-1}.

To elucidate any electronic changes in the catalyst, XPS measurements were conducted. The Al2p and O1s lines remain unchanged (see Figure S7, Figure S8), while a few changes in electronic nature of platinum and phosphorus are observable. The Pt4d line of the unmodified Pt catalyst (**1-a**) is located at 314.8 eV (Fig. 6 a), which can be assigned to Pt^0.[25–27] The P-modified Pt catalyst (**2**) after impregnation with the phosphorus precursor and before reduction exhibits a shift of the respective line to higher binding energies (315.4 eV). This is due to the presence of additional oxidized Pt^{2+}.[28] This species is formed upon calcination at 400 °C of the Pt-impregnated catalyst due to the decomposition of $H_2[PtCl_6]$ to $PtCl_2$.[29,30] Upon reduction of the P-modified Pt catalyst, the Pt4d lines shift to the same binding energies of Pt^0 as in the unmodified counterpart. The comparison of P-modified catalysts with different molar P:Pt ratios (Fig. 6 b) shows no significant

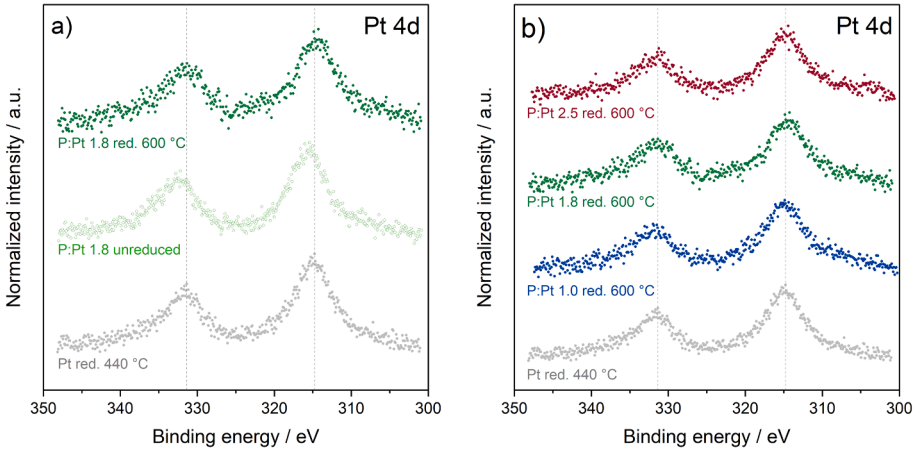

Fig. 6. XPS spectra of Pt 4d line. a) Unmodified Pt catalyst (**1-a**) and unreduced and reduced P-modified Pt catalyst (**2**). b) Unmodified Pt catalyst (**1-a**) and P-modified Pt catalysts with molar P:Pt ratios of 1.0, 1.8 and 2.5 (catalyst **2-a**, **2** and **2–b**).

differences in the Pt4d line. In all cases Pt is mainly present as Pt^0.

The P2p line of the P-modified Pt catalyst is located at 134.0 eV before and at 134.4 eV after reduction at 600 °C (Fig. 7 a). These binding energies are indicative of oxidized phosphorus species like phosphates such as $AlPO_4$.[31–33] Species with even higher oxidation states such as P_2O_5 or H_3PO_4 would be expected above 135 eV,[19,33,34] while the most common platinum phosphide PtP_2 would show a signal at binding energies < 130 eV [25,35,36] due to a high electron density at phosphorus. No significant differences in the P2p line for Pt-P catalysts with different P:Pt ratios were observed (Fig. 7 b).

For analysis of the crystalline phases present in the catalyst materials, XRD investigations of unmodified Pt catalysts as well as Pt-P catalysts with different molar P:Pt ratios were performed (Fig. 8). All diffractograms are dominated by reflections of the γ-Al_2O_3 support (black) that overlap with most of the Pt reflections[37]. The unmodified Pt catalyst reduced at 600 °C (**1-b**) exhibits a Pt(0) reflection at approximately 80°, that is not visible for the sample reduced at 440 °C (**1-a**). The same Pt reflection becomes visible in the phosphorus-modified samples for higher molar P:Pt ratios of 2.5 and 4.2 (catalysts **2-b** and **2-c**), while being absent in the samples with P:Pt ratios of 1.0 and 1.8 (catalysts **2-a** and **2**). A sharper reflection occurs at 39° for the same samples that also originates from platinum but is overlapped by γ-Al_2O_3.

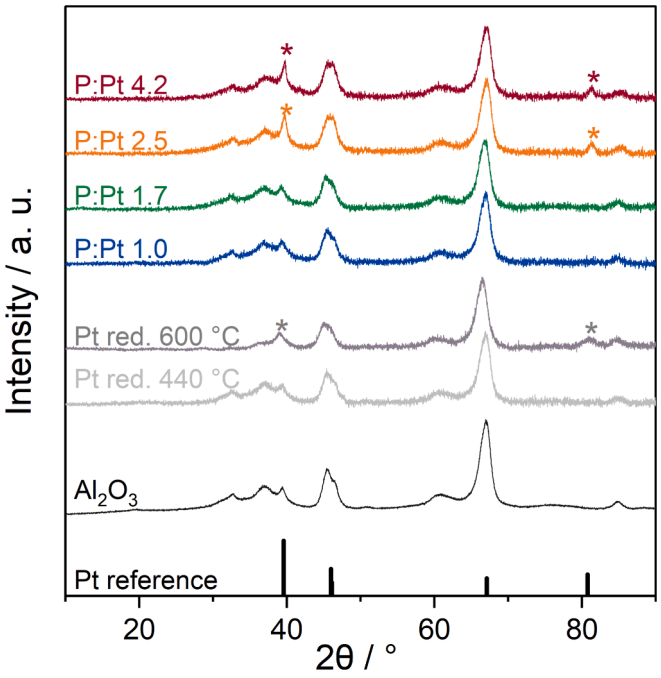

Fig. 8. XRD patterns of Al_2O_3 support, unmodified Pt catalysts reduced at 440 and 600 °C (catalysts **1-a** and **1-b**) and phosphorus-modified Pt catalysts (reduced at 600 °C) with molar P:Pt ratios of 1.0, 1.8, 2.5, and 4.2 (catalysts **2-a**, **2**, **2-b** and **2-c**) and platinum metal reference.

4. Discussion

In this study, we aimed for answering the question whether P-modification of a Pt/Al_2O_3 dehydrogenation catalyst proceeds in a similar manner to the literature-known S-modification. Regarding the modification step itself, a distinct difference is apparent. For all prepared P-modified Pt catalysts, the nominal Pt and P loadings could be achieved without any loss of phosphorus upon reduction at temperatures of up to 900 °C (catalyst **3-f**). Consequently, an easily applicable approach for P-modification of Pt/Al_2O_3 catalysts was developed that allows a reliable adjustment of the catalyst composition. In the case of S-modification, only 50 % of the nominal sulfur loading is found on the catalyst after reduction at only 440 °C (Table S2). The reason behind this sulfur loss is a partial decomposition and removal of surface sulfate species upon reduction in form of H_2S, especially at high temperatures and loadings. [15,38,39] We have shown here, that the phosphorus promoter is preserved on the catalyst even at elevated temperatures, with improved catalytic properties for dehydrogenation of perhydro benzyltoluene. Consequently, the stability of phosphorus on the P-modified catalyst marks a significant difference and advantage over the known S-modification.

In the catalytic testing of the P-modified samples, an increase in H_2 yield by 18 % was found for catalyst **2**, having a P:Pt ratio of 1.8, compared to unmodified catalyst **1-a**. This corresponds to an optimum P loading of 0.9 wt% and a coverage of 1.2 P_{atoms} per nm^2 for the case of 3 wt% Pt loading, as investigated in our study. Note that when the Pt content or support characteristics are altered, it must be assumed that the P:Pt ratio alone might not be decisive, but the total phosphorus loading as well as coverage should also be taken into account. As the side product methyl fluorene is formed by releasing a further hydrogen molecule in the described deep dehydrogenation step, it appears logical that its production is also enhanced by the more active, P-modified catalyst. While the unmodified Pt catalyst showed a significantly reduced dehydrogenation activity upon an increase in reduction temperature from 440 to 600 °C, the P-modified catalysts require a minimum of 550 °C for a significant activity boost. Interestingly, catalysts showed a similarly high dehydrogenation activity after reduction at even 900 °C, demonstrating the high temperature stability of these Pt-P/

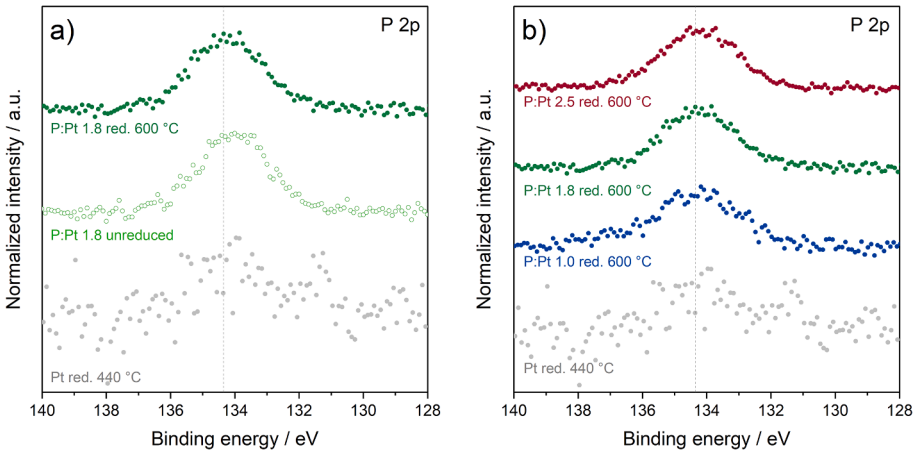

Fig. 7. XPS spectra of P 2p line. a) Unmodified Pt catalyst (**1-a**) and unreduced and reduced P-modified Pt catalyst (**2**). b) Unmodified Pt catalyst (**1-a**) and P-modified Pt catalysts with molar P:Pt ratios of 1.0, 1.8, and 2.5 (catalyst **2-a**, **2** and **2–b**).

Al_2O_3 catalysts. It is well known for Pt/Al_2O_3 catalysts, that high temperatures can provoke a reduction of the active metal surface area due to formation of larger platinum particles by sintering, which makes P-modification a powerful tool to stabilize metal dispersion.[40,41].

Our STEM measurements indeed demonstrate a severe sintering effect for unmodified Pt catalysts leading to a fivefold increase of average particle size when a reduction temperature of 600 °C instead of 440 °C is applied. The drastically reduced CO chemisorption capacity of the unmodified Pt catalyst upon this elevated reduction temperature is well in line with these findings as the increased platinum particle size obtained after the reduction at 600 °C reduces the number of CO binding sites on the Pt surface.[41] Furthermore, XRD measurements showed that the reflection attributed to elemental Pt at approximately 80° becomes visible after the 600 °C treatment of the unmodified Pt/Al_2O_3 due to the formation of sufficiently large and crystalline Pt particles, while it was absent in the case of 440 °C. The strong sintering of the Pt particles that occurs during reduction at 600 °C if a P-modification is not applied proven by STEM, CO chemisorption and XRD, explains the deteriorated dehydrogenation activity of this catalyst.

For the P-modified catalyst **2** on the other hand, STEM-EDX spectrum imaging demonstrated that Pt and P are homogeneously distributed across the surface of the support. Note, that the atomic diameter of a platinum atom is about 0.274 nm.[42] Accordingly, Pt clusters consisting of only few atoms are present after catalyst treatment at high temperatures of 600 °C, if our P-modification approach was applied. These particles are too small to cause sufficient scattering to be visible in our XRD measurement. Consequently, the phosphorus addition stabilizes the Pt nanoparticles and even slightly improves their dispersion. Due to identical catalyst activity after treatments at 600 °C and 900 °C, this stabilizing effect remains even at high temperatures. We therefore propose that the phosphorus species on the catalyst act as anchoring sites for the Pt particles on the Al_2O_3 surface, thereby reducing their mobility. STEM-EDX scans of few larger particles present on P-modified catalysts at non-optimal P:Pt ratio support the proposed close interaction of phosphorus and platinum, as P is especially concentrated at the Pt nanoparticles. From this we conclude that P is preferably located in the proximity of Pt even for the highly dispersed particles of smaller size (1 nm).

If the sample is reduced at temperatures below 550 °C, the activity of the P-modified sample was below its unmodified counterpart. Comparing Pt-P catalysts reduced below (440 °C) and above (600 °C) this temperature in CO chemisorption measurements, an increase in CO adsorption capacity after the high temperature treatment becomes apparent. The sample reduced at 440 °C might have a lower CO adsorption capacity due to a pronounced blockage of platinum centers by P species. It is also interesting to note that the optimally P-modified catalyst **2** has a lower CO adsorption capacity than the unmodified catalyst **1-a** despite its higher dehydrogenation activity. In this context, a reduced CO adsorption capacity of P-modified catalysts due to larger particles can be excluded, based on the STEM results. Considering the available Pt surface (from particle sizes visible in STEM) and the measured low CO adsorption capacity of the P-modified catalyst **2**, this hints to a partial blockage of Pt sites by phosphorus, that still occurs, but to a lower extent after 600 °C treatment. Potentially, the Pt atoms at the interphase of the particle and the Al_2O_3 support are interacting with the phosphorous "anchor species" and are therefore not accessible for reactants. At a lower P:Pt ratio of 1.0, despite the slightly higher CO adsorption capacity, a lower catalytic activity was observed. Supposedly, if the amount of phosphorus is too low, the promoter cannot fully develop its positive effect on all active platinum. For this non-optimal case, highly dispersed Pt particles of ca. 1 nm are observed along with a few larger particles with diameters above 5 nm in our STEM examinations (Figure S4), showing that CO adsorption capacity is not the only decisive factor. Thus, too low phosphorus loading only stabilizes a part of the Pt nanoparticles, while others not in contact with phosphorus still undergo sintering. At higher P:Pt ratios than the optimum (P:Pt 2.5 and 4.2), CO adsorption capacity was reduced by approximately 37 % with respect to catalyst **2** (P:Pt 1.8). This shows that additional Pt sites are blocked by phosphorus, when exceeding the optimum P loading. Taking these results together with the enhanced activity in dehydrogenation and higher stability of the catalyst at optimum P loading, we suggest a strong interaction and spatial proximity of platinum and phosphorus. Furthermore, the increased activity, despite a partial coverage of the highly disperse Pt particles by P species, implies a significant increase of the intrinsic activity per available Pt center upon P-modification. Here, the initial H_2 productivity per available Pt (determined *via* the dispersion from CO chemisorption) for the optimum P:Pt ratio of 1.8 is approximately even 33 % higher than for unmodified catalyst **1-a** and is on a higher level compared to all other catalysts throughout the course of reaction (Figure S11 b). From other dopants than P it is known that electron transfer to the Pt atoms lowers CO binding energies and modifies CO coordination.[43] Electronic effects of this kind could also occur through P-modification and explain the simultaneously higher catalytic activity and lower CO adsorption capacity of the respective catalysts.

Overall, P-modification has shown to be an excellent strategy to improve and stabilize catalytic activity, even during high temperature treatment or application of the catalysts. Our studies reveal that the maximum activity boost in perhydro benzyltoluene dehydrogenation by P-modification of the catalysts only becomes effective if a P:Pt ratio of about 1.8 (1.2 P_{atoms}/nm^2) is applied. Apart from a too low P content, a similar mixture of small, stabilized nanoparticles and large clusters with sizes > 5 nm was also observed in the catalyst with a too high P content (P:Pt ratio > 1.8). Furthermore, catalyst **2-b** with a P:Pt ratio of 2.5 showed the characteristic Pt reflection at 80° in the XRD measurements, that we assume to be only present if larger Pt clusters are present in the sample. In samples with too high P:Pt ratio, besides the blockage of further Pt sites, the entire amount of phosphorus might not be available for stabilization, which means that sintering of some of the nanoparticles is not prevented. Since an increase of P:Pt ratio from 2.5 to 4.2 did not further reduce the CO adsorption capacity of the catalyst, this hints to the deposition of phosphorus on the support – not affecting the Pt active sites – e.g. by the formation of polyphosphates at too high phosphorus loading.[44] Similar observations were also made with Pd catalysts supported on P-modified Al_2O_3.[45] Phosphorus consumed by polyphosphate formation is no longer available for stabilizing the metal nanoparticles. In addition, too high amounts of phosphorus and polyphosphate species might increasingly block active platinum sites, which also results in a loss of dehydrogenation activity.

XPS measurements revealed no significant changes in the Al2p and O1s lines. The Pt4d line of the unmodified Pt catalyst (**1-a**) is assigned to Pt^0 according to literature[25–27] while the P-modified Pt catalyst (**2**) before reduction exhibits a shift of the respective line to higher binding energies – indicating the presence of additional oxidized Pt^{2+} formed upon calcination[28–30]. Upon reduction of the P-modified Pt catalyst, the Pt4d lines shift to the same binding energies of Pt^0 as in the unmodified counterpart. These results show that our P-modification method not only preserves small Pt particle sizes (as observed by STEM), but at the same time keeps platinum in a reduced state. This is significantly different from the SiO_2-supported PtP_2-phase studied by Kou *et al.*, where a clear shift of the Pt4f line to higher binding energies (formation of Pt^{2+}) was observed. Here, the oxidation of Pt upon formation of a phosphide phase is accompanied by a severe loss in dehydrogenation activity.[19] The absence of Pt^{2+} in our P-modified catalyst further hints to an absence of platinum phosphide (PtP_2)[19,46], which is in accordance with the absence of any platinum phosphide crystal phases in our XRD measurements. For different molar P:Pt ratios no significant differences in the Pt4d lines could be observed, showing that Pt^0 is the main platinum species. Consequently, phosphorus does not seem to change the platinum oxidation state, but alters its CO adsorption behavior and additionally acts as a structural promoter to platinum.

The P2p line of the P-modified Pt catalyst shifts to slightly higher binding energies upon reduction at 600 °C which are indicative of

oxidized phosphorus species like phosphates[31–33] whereas phosphide species (expected binding energy < 130 eV [25,35,36]) cannot be observed even at high P loadings. Due to the sensitivity of XPS, the presence of a phosphide phase cannot be excluded with full certainty as Kou *et al.* could also not observe a binding energy typical for phosphides in the XPS-spectra of the P2p line. However, the authors could prove the presence of PtP_2 with XRD for their material[19], while the respective reflections are not visible in our study. Despite a reducing atmosphere during the last preparation step, the P2p line is shifted to higher binding energy, which is equivalent to a loss in electron density at the phosphorus atom. A hypothesis for this shift might be that there is no electron transfer from platinum to phosphorus (which would be expected for the formation of phosphides), but rather in the opposite direction, from phosphorus to platinum, which hints to a close interaction between the two elements. This is in line with the observations from the Pt4d line, where the main platinum species for all P-modified catalysts is Pt^0. This subtle shift in binding energy observed for the P2p line is not visible for the Pt4d line, as the H_2/N_2 atmosphere during the final synthesis step would transform platinum to its reduced state Pt^0 also without P-modification (catalyst **1-a**). Yet, we consider Pt to be a possible acceptor of electron density from phosphorus, which is supported by the close interaction between the two elements observed in STEM-EDX and altered CO chemisorption properties. Since no differences are visible in XPS for different P loadings, we further suggest that the electron density shift alone cannot be responsible for an enhanced catalytic activity, but rather a combination with particle sizes and P coverage on the catalyst surface. From the presence of oxidized phosphorus species, we suggest that phosphates are bound to the Al_2O_3 support restricting their mobility. As the results from STEM-EDX, CO pulse chemisorption and the shifts in binding energy of Pt4d and P2p lines hint to a strong interaction and proximity of platinum and phosphorus, the immobile phosphate species seem to stabilize the dispersion of Pt nanoparticles and hinder their sintering. Further analytical investigations are intended in a follow-up work for a deeper understanding of these catalyst systems.

5. Conclusion

In this study, we presented novel phosphorus-modified platinum catalysts and discussed the effects of phosphorus-modification on the physicochemical and catalytic properties. 3 wt% Pt on Al_2O_3 catalysts were modified with phosphorus by wet impregnation using H_3PO_3. With respect to catalytic activity in the targeted dehydrogenation of perhydro benzyltoluene, a molar P:Pt ratio of 1.8 was found optimal. The highest H_2 yields are achieved when the P-modified catalysts were reduced at 550 °C or higher with no decrease in performance being observed when the reduction temperature is further increased up to 900 °C. The obtained catalysts exhibit very attractive dehydrogenation activity (increase by up to 18 % compared to the unmodified Pt catalyst). This high dehydrogenation activity is further reflected by the higher formation of methyl fluorene, which forms in a consecutive dehydrogenation from benzyltoluene (deep dehydrogenation). The phosphorus-modified platinum catalysts have narrower particle size distributions and smaller average particle sizes compared to pure platinum catalysts reduced at lower temperatures (440 °C instead of 600 °C), showing the dispersion-stabilizing effect of the P-modification. Furthermore, STEM-EDX scans have shown that phosphorus is preferably located at the Pt nanoparticles, indicating a close interaction between the two elements. A decreased CO adsorption capacity of the most active Pt-P catalyst with the smallest particle size hints to an additional electronic effect of the phosphorus additive on platinum. XPS measurements have shown that Pt is still in its reduced state after P-modification and no phosphide phase is formed, which is an important factor for high dehydrogenation activity. Despite the reducing conditions during the high-temperature treatment of the catalyst, phosphorus experiences a loss in electron density, while Pt is reduced to Pt^0. XRD diffractograms of the catalysts did not show crystalline phases of platinum phosphide even at high P:Pt ratios and after reduction procedures at up to 900 °C where unmodified Pt on alumina shows severe sintering. This indicates that the here-presented P-modification provides a synthetically simple and very effective way to stabilize Pt nanoparticles below 2 nm particle size on alumina supports even under very harsh pretreatment and reaction conditions.

CRediT authorship contribution statement

Abelina Ellert: Writing – original draft, Visualization, Investigation, Conceptualization. **Felix Herold:** Investigation. **Magnus Rønning:** Writing – review & editing, Funding acquisition. **Andreas Hutzler:** Investigation. **Luca Piccirilli:** Investigation. **Ton V.W. Janssens:** Writing – review & editing, Project administration. **Peter N.R. Vennestrøm:** Project administration. **Peter Wasserscheid:** Writing – review & editing, Supervision, Funding acquisition. **Patrick Schühle:** Writing – review & editing, Supervision, Conceptualization.

Declaration of competing interest

The authors declare the following financial interests/personal relationships which may be considered as potential competing interests: Patrick Schuehle, Abelina Ellert, Ton Janssens, Peter Wasserscheid has patent pending to Umicore SA. If there are other authors, they declare that they have no known competing financial interests or personal relationships that could have appeared to influence the work reported in this paper.

Data availability

Research data to this article can be found online at https://doi.org/10.5281/zenodo.11144621.

Acknowledgment

FH acknowledges a fellowship within the Walter-Benjamin-program of the Deutsche Forschungsgemeinschaft (DFG, German Research Foundation, project number 471263729). The Research Council of Norway is acknowledged for the support to the Norwegian Micro- and Nano-Fabrication Facility, NorFab, project number 295864. Umicore Denmark ApS is acknowledged for funding of this research.

Appendix A. Supplementary data

Supplementary data to this article can be found online at https://doi.org/10.1016/j.jcat.2024.115607.

References

[1] B.D. Chandler, L.I. Rubinstein, L.H. Pignolet, Alkane dehydrogenation with silica supported platinum and platinum-gold catalysts derived from phosphine ligated precursors, J. Mol. Catal. A Chem. 133 (3) (1998) 267–282, https://doi.org/10.1016/S1381-1169(97)00281-1.

[2] F. Auer, A. Hupfer, A. Bösmann, N. Szesni, P. Wasserscheidpeter, Influence of the nanoparticle size on hydrogen release and side product formation in liquid organic hydrogen carrier systems with supported platinum catalysts, Catal. Sci. Technol. 10 (19) (2020) 6669–6678, https://doi.org/10.1039/D0CY01173H.

[3] S. Nagatake, T. Higo, S. Ogo, Y. Sugiura, R. Watanabe, C. Fukuhara, Y. Sekine, Dehydrogenation of Methylcyclohexane over Pt/TiO2 Catalyst, Catal. Lett. 146 (1) (2016) 54–60, https://doi.org/10.1007/s10562-015-1623-3.

[4] J. Oh, Y. Jo, T.W. Kim, H.B. Bathula, S. Yang, J.H. Baik, Y.-W. Suh, Highly efficient and robust Pt ensembles on mesoporous alumina for reversible H2 charge and release of commercial benzyltoluene molecules, Appl. Catal. B 305 (2022) 121061, https://doi.org/10.1016/j.apcatb.2022.121061.

[5] W. Yu, M.D. Porosoff, J.G. Chen, Review of Pt-based bimetallic catalysis: from model surfaces to supported catalysts, Chem. Rev. 112 (11) (2012) 5780–5817, https://doi.org/10.1021/cr300096b.

[6] X. Zhang, N. He, L. Lin, Q. Zhu, G. Wang, H. Guo, Study of the carbon cycle of a hydrogen supply system over a supported Pt catalyst: methylcyclohexane–toluene–hydrogen cycle, Catal. Sci. Technol. 10 (4) (2020) 1171–1181, https://doi.org/10.1039/C9CY01999E.

[7] K. Alconada, V.L. Barrio, Evaluation of bimetallic Pt–Co and Pt–Ni catalysts in LOHC dehydrogenation, Int. J. Hydrogen Energy (2023), https://doi.org/10.1016/j.ijhydene.2023.04.120.

[8] J.K. Dunleavy, Sulfur as a catalyst poison, Platinum Met. Rev. 50 (2) (2006) 110, https://doi.org/10.1595/147106706X111456.

[9] M. Argyle, C. Bartholomew, Heterogeneous catalyst deactivation and regeneration: a review, Catalysts 5 (1) (2015) 145–269, https://doi.org/10.3390/catal5010145.

[10] L. Deng, H. Miura, T. Shishido, Z. Wang, S. Hosokawa, K. Teramura, T. Tanaka, Elucidating strong metal-support interactions in Pt–Sn/SiO2 catalyst and its consequences for dehydrogenation of lower alkanes, J. Catal. 365 (2018) 277–291, https://doi.org/10.1016/j.jcat.2018.06.028.

[11] A. Virnovskaia, S. Morandi, E. Rytter, G. Ghiotti, U. Olsbye, Characterization of Pt, Sn/Mg(Al)O catalysts for light alkane dehydrogenation by FT-IR spectroscopy and catalytic measurements, J. Phys. Chem. C 111 (40) (2007) 14732–14742, https://doi.org/10.1021/jp074686u.

[12] A.J. McCue, J.A. Anderson, Sulfur as a catalyst promoter or selectivity modifier in heterogeneous catalysis, Catal. Sci. Technol. 4 (2) (2014) 272–294, https://doi.org/10.1039/C3CY00754E.

[13] G.M. Bickle, J. Biswas, D.D. Do, Role of sulphur in catalytic reforming of hydrocarbons on platinum/alumina, Appl. Catal. 36 (1988) 259–276, https://doi.org/10.1016/S0166-9834(00)80120-7.

[14] M. Wilde, T. Stolz, R. Feldhaus, K. Anders, The influence of sulfur on activity and selectivity of reforming catalysts in the conversion of individual hydrocarbons, Appl. Catal. 31 (1) (1987) 99–111, https://doi.org/10.1016/S0166-9834(00)80669-7.

[15] F. Auer, D. Blaumeiser, T. Bauer, A. Bösmann, N. Szesni, J. Libuda, P. Wasserscheid, Boosting the activity of hydrogen release from liquid organic hydrogen carrier systems by sulfur-additives to Pt on alumina catalysts, Catal. Sci. Technol. 9 (13) (2019) 3537–3547, https://doi.org/10.1039/C9CY00817A.

[16] Q.N. Dao, E. On, S. Ramadhani, K. Lee, H. Sohn, S.H. Choi, S.Y. Lee, H. Jeong, Y. Kim, Catalytic insights into perhydro-benzyltoluene dehydrogenation: probing surface characteristics revealed by DRIFTS study, Int. J. Hydrogen Energy 56 (2024) 1284–1293, https://doi.org/10.1016/j.ijhydene.2023.12.254.

[17] A. Gutierrez, R.K. Kaila, M.L. Honkela, R. Slioor, A.O.I. Krause, Hydrodeoxygenation of guaiacol on noble metal catalysts, Catal. Today 147 (3) (2009) 239–246, https://doi.org/10.1016/j.cattod.2008.10.037.

[18] C.N.M. Ouma, K.O. Obodo, P.M. Modisha, D. Bessarabov, Si, P, S and Se surface additives as catalytic activity boosters for dehydrogenation of methylcyclohexane to toluene - a liquid organic hydrogen carrier system: density functional theory insights, Mater. Chem. Phys. 279 (2022) 125728, https://doi.org/10.1016/j.matchemphys.2022.125728.

[19] J. Kou, J. Zhu Chen, J. Gao, X. Zhang, J. Zhu, A. Ghosh, W. Liu, A.J. Kropf, D. Zemlyanov, R. Ma, X. Guo, A.K. Datye, G. Zhang, L. Guo, J.T. Miller, Structural and Catalytic Properties of Isolated Pt^{2+} Sites in Platinum Phosphide (PtP_2), ACS Catal. 11 (21) (2021) 13496–13509, https://doi.org/10.1021/acscatal.1c03970.

[20] M. Kärkkäinen, T. Kolli, M. Honkanen, O. Heikkinen, M. Huuhtanen, K. Kallinen, T. Lepistö, J. Lahtinen, M. Vippola, R.L. Keiski, The effect of phosphorus exposure on diesel oxidation catalysts—Part I: activity measurements, elementary and surface analyses, Top. Catal. 58 (14–17) (2015) 961–970, https://doi.org/10.1007/s11244-015-0464-z.

[21] T. Solymosi, F. Auer, S. Dürr, P. Preuster, P. Wasserscheid, Catalytically activated stainless steel plates for the dehydrogenation of perhydro dibenzyltoluene, Int. J. Hydrogen Energy 46 (70) (2021) 34797–34806, https://doi.org/10.1016/j.ijhydene.2021.08.040.

[22] B. Isaacs, The effect of drying temperature on the temperature-programmed reduction profile of a platinum/rhenium/alumina catalyst, J. Catal. 77 (1) (1982) 43–52, https://doi.org/10.1016/0021-9517(82)90144-0.

[23] H. Jorschick, M. Geißelbrecht, M. Eßl, P. Preuster, A. Bösmann, P. Wasserscheid, Benzyltoluene/dibenzyltoluene-based mixtures as suitable liquid organic hydrogen carrier systems for low temperature applications, Int. J. Hydrogen Energy 45 (29) (2020) 14897–14906, https://doi.org/10.1016/j.ijhydene.2020.03.210.

[24] D. Strauch, P. Weiner, B.B. Sarma, A. Körner, E. Herzinger, P. Wolf, A. Zimina, A. Hutzler, D.E. Doronkin, J.-D. Grunwaldt, P. Wasserscheid, M. Wolf, Bimetallic platinum rhenium catalyst for efficient low temperature dehydrogenation of perhydro benzyltoluene, Catal. Sci. Technol. (2024), https://doi.org/10.1039/D3CY01336G.

[25] J.F. Moulder, Handbook of X-Ray Photoelectron Spectroscopy: A Reference Book of Standard Spectra for Identification and Interpretation of XPS Data, Perkin-Elmer Corporation, Physical Electronics Division, 1992.

[26] G. Schön, High resolution auger electron spectroscopy of metallic copper, J. Electron Spectrosc. Relat. Phenom. 1 (4) (1972) 377–387, https://doi.org/10.1016/0368-2048(72)80039-2.

[27] W.-D. Schneider, C. Laubschat, Actinide—noble-metal systems: an x-ray-photoelectron-spectroscopy study of thorium-platinum, uranium-platinum, and uranium-gold intermetallics, Phys. Rev. B 23 (3) (1981) 997–1005, https://doi.org/10.1103/PhysRevB.23.997.

[28] S.D. Jackson, J. Willis, G.D. Mclellan, G. Webb, M.B.T. Keegan, R.B. Moyes, S. Simpson, P.B. Wells, R. Whyman, Supported metal catalysts: preparation, characterization, and function, J. Catal. 139 (1) (1993) 191–206, https://doi.org/10.1006/jcat.1993.1017.

[29] K. Kinoshita, K. Routsis, J.A.S. Bett, The thermal decomposition of platinum (II) and (IV) complexes, Thermochim. Acta 10 (1) (1974) 109–117, https://doi.org/10.1016/0040-6031(74)85029-X.

[30] A.E. Schweizer, G.T. Kerr, Thermal decomposition of hexachloroplatinic acid, Inorg. Chem. 17 (8) (1978) 2326–2327, https://doi.org/10.1021/ic50186a067.

[31] T. Lindblad, B. Rebenstorf, Z.-G. Yan, S.L.T. Andersson, Characterization of Vanadia supported on amorphous AlPO4 and its properties for oxidative dehydrogenation of propane, Appl. Catal. A 112 (2) (1994) 187–208, https://doi.org/10.1016/0926-860X(94)80219-X.

[32] J.A. Rotole, P.M.A. Sherwood, Aluminum Phosphate by XPS, Surf. Sci. Spectra 5 (1) (1998) 60–66, https://doi.org/10.1116/1.1247858.

[33] E. Fluck, D. Weber, Anwendung der Röntgen-Photoelektronenspektroskopie in der Phosphorchemie, II: P $_{2p}$ -Bindungsenergien in Phosphor(III)-Verbindungen, Phosphoniumsalzen und Sauerstoffsäuren des Phosphors / P $_{2p}$ Binding Energies in Phosphorus(III) Compounds, Phosphonium Salts and Oxyacids of Phosphorus, Zeitschrift Für Naturforschung B 29 (9–10) (1974) 603–607, https://doi.org/10.1515/znb-1974-9-1006.

[34] R. Nishitani, H. Iwasaki, Y. Mizokawa, S. Nakamura, An XPS analysis of thermally grown oxide film on GaP, Jpn. J. Appl. Phys. 17 (2) (1978) 321–327, https://doi.org/10.1143/JJAP.17.321.

[35] S.H. Baker, S.C. Bayliss, S.J. Gurman, N. Elgun, E.A. Davis, A Structural and Optical Study of Sputtered InP Films as a Function of Preparation Temperature, J. Phys.: Condens. Matter 8 (10) (1996) 1591–1605, https://doi.org/10.1088/0953-8984/8/10/028.

[36] U. Elrod, M.C. Lux-Steiner, M. Obergfell, E. Bucher, L. Schlapbach, Surface chemistry of Zn3P3 single crystals studied by XPS, Appl. Phys. B 43 (3) (1987) 197–201, https://doi.org/10.1007/BF00695623.

[37] G. Bredig, R. Allolio, Röntgenuntersuchungen an Katalytisch Wirkenden Metallen, Z. Phys. Chem. 126U (1) (1927) 41–71, https://doi.org/10.1515/zpch-1927-12604.

[38] J.M. Parera, C.R. Aspesteguia, Sulfurization of Pt/Al_2O_3-Cl Catalysts. I. Adsorption Isotherms.

[39] C.R. Apesteguía, J. Barbier, The role of catalyst presulfurization in some reactions of catalytic reforming and hydrogenolysis, J. Catal. 78 (2) (1982) 352–359, https://doi.org/10.1016/0021-9517(82)90319-0.

[40] W.G. Rothschild, H.C. Yao, H.K. Plummer, Surface Interaction in the Platinum-.Gamma.-Alumina System. V. Effects of atmosphere and fractal topology on the sintering of platinum, Langmuir 2 (5) (1986) 588–593, https://doi.org/10.1021/la00071a010.

[41] Y. Chu, On the sintering of platinum on alumina model catalyst, J. Catal. 55 (3) (1978) 281–298, https://doi.org/10.1016/0021-9517(78)90217-8.

[42] E. Wiberg, N. Wiberg, Lehrbuch der anorganischen Chemie, 102., stark umgearbeitete und verbesserte Auflage.; A. F. Holleman, G. Fischer, (Eds.), Walter de Gruyter: Berlin New York, 2007.

[43] P. Ferrari, L.M. Molina, V.E. Kaydashev, J.A. Alonso, P. Lievens, E. Janssens, Controlling the adsorption of carbon monoxide on platinum clusters by dopant-induced electronic structure modification, Angew Chem Int Ed 55 (37) (2016) 11059–11063, https://doi.org/10.1002/anie.201604269.

[44] A. Morales, M.M.R. De Agudelo, F. Hernández, Adsorption mechanism of phosphorus on alumina, Appl. Catal. 41 (1988) 261–271, https://doi.org/10.1016/S0166-9834(00)80397-8.

[45] J. Dong, J. Wang, J. Wang, M. Yang, W. Li, M. Shen, Enhanced thermal stability of palladium oxidation catalysts using phosphate-modified alumina supports, Catal. Sci. Technol. 7 (21) (2017) 5038–5048, https://doi.org/10.1039/C7CY01534H.

[46] W. Tian, Y. Wang, W. Fu, J. Su, H. Zhang, Y. Wang, PtP $_2$ Nanoparticles on N, P doped carbon through a self-conversion process to core-shell Pt/PtP 2 as an efficient and robust ORR catalyst, J. Mater. Chem. A 8 (39) (2020) 20463–20473, https://doi.org/10.1039/D0TA06566H.